2019 IEEE 9th International Conference on Nanomaterials: Applications & Properties (NAP – 2019)
Odesa, Ukraine, September 15-20, 2019

Ministry of Education and Science of Ukraine
Sumy State University
IEEE Nanotechnology Counsil
IEEE Magnetic Society
The International Union of Pure and Applied Physics

Proceedings of the 2019 IEEE 9th International Conference on Nanomaterials: Applications & Properties (NAP-2019)

NANOmaterials: Applications & Properties-2019

Part 2

ISBN 978-1-7281-2830-6

Sumy
Sumy State University
2019

Ministry of Education and Science of Ukraine
Sumy State University
IEEE Nanotechnology Council
IEEE Magnetics Society
The International Union of Pure and Applied Physics

Proceedings of the 2019 IEEE 9th International Conference on Nanomaterials: Applications & Properties (NAP-2019)

2019, Part 2

Odesa, Ukraine
September 15–20, 2019

Founded in 2011

Sumy
Sumy State University
2019

2019 IEEE 9th International Conference on Nanomaterials: Applications & Properties (NAP – 2019)

IEEE Catalog Number: CFP19F65-ART
ISBN: 978-1-7281-2830-6

Sumy State University
2, Rymskogo-Korsakova St.,
40007 Sumy, Ukraine

SUMY STATE UNIVERSITY

Proceedings of the 2019 IEEE 9th International Conference on Nanomaterials: Applications & Properties (NAP-2019)

2019, Part 2

COMMITTEES

ORGANIZING COMMITTEE

INTERNATIONAL SCIENTIFIC COMMITTEE

Vladimir Cambel	Institute of Electrical Engineering, Slovak Academy of Sciences (Slovakia)
Vadym Zayets	Spintronics Research Center, National Institute of Advanced Industrial Science and Technology (AIST) (Japan)
Pavlo Mikheenko	University of Oslo (Norway)
Goran Karapetrov	Drexel University (USA)
Oleksandr Bondar	Sumy State University (Ukraine)
Motoki Ota	Metallurgical Research Laboratory, Hitachi Metals Ltd. (Japan)
Vladimir Komanicky	Institute of Physics, Pavol Jozef Safarik University (Slovakia)
Fedir Sizov	V.E. Lashkaryov Institute of Semiconductor Physics NAS of Ukraine (Ukraine)

LOCAL ORGANIZING COMMITTEE

Alexander Pogrebnjak	Sumy State University (Ukraine)
Valentyn Novosad	Argonne National Laboratory (USA)
Serhiy Protsenko	Sumy State University (Ukraine)
Yurii Shabelnyk	Sumy State University (Ukraine)
Aleksey Drozdenko	Sumy State University (Ukraine)
Kateryna Smyrnova	Sumy State University (Ukraine)
Vlad Rogoz	Sumy State University (Ukraine)
Yaroslav Kravchenko	Sumy State University (Ukraine
Oleksandr Bondar	Sumy State University (Ukraine)
Anna Marchenko	Sumy State University (Ukraine)
Artem Bagdasaryan	Sumy State University (Ukraine)
Margaryta Lisovenko	Sumy State University (Ukraine)

ORGANIZERS

MINISTRY OF EDUCATION AND SCIENCE OF UKRAINE

SUMY STATE UNIVERSITY

IEEE

DREXEL UNIVERSITY

SPONSORS

IEEE NANOTECHNOLOGY COUNCIL

IEEE MAGNETICS SOCIETY

THE INTERNATIONAL UNION OF PURE AND APPLIED PHYSICS

KAUFMAN & ROBINSON, INC.

OPTEC GROUP

K-TEK NANOTECHNOLOGY, LLC

ANGSTROM ENGINEERIN, INC.

AJA INTERNATIONAL, INC.

BRUKER

MEDIA PARTNERS

EUROPEAN MAGNETISM ASSOCIATION

SPRINGER NATURE

IEEE XPLORE DIGITAL LIBRARY

JOURNAL OF NANO- AND ELECTRONIC PHYSICS

ACS NANO

Table of Contents

2019, Part 2

Track: Biomedical Applications

Track: Theory & Modeling

Composite Ultrafiltration Membrane Incorporated with Dispersed Oxide Nanoparticles

Liudmyla M. Rozhdestvenska
Laboratory of sorption & membrane materials & technologies
Vernadsky Institute of general and inorganic chemistry of the Ukrainian National Academy of Sciences
Kyiv, Ukraine
ludar777@ukr.net

Liudmyla N. Ponomarova
Department of Theoretical and Applied Chemistry
Sumy State University
Sumy, Ukraine
l.ponomarova@chem.sumdu.edu.ua

Alexander V. Bilduykevich
Laboratory of membrane processes, Institute of Physical Organic Chemistry of the National Academy of Science of Belarus
Minsk, Belarus
uf@ifoch.bas-net.by

Oleg I. V'yunov
Department of solid state chemistry, Vernadsky Institute of general and inorganic chemistry of the Ukrainian National Academy of Sciences
Kyiv, Ukraine
vyunov@ukr.net

Viktoria D. Ivchenko
Department of Theraphy, Pharmakology, Clinical diagnostick and Chemistry
Sumy National Agrarian University
Sumy, Ukraine
ivchenkovd@gmail.com

Yurii G. Zmievskii
Department of technological equipment and computer technology design qualifies National University of Food Technologies of the Ministry of Education and Science of Ukraine
Kyiv, Ukraine
yrazm@meta.ua

***Abstract* — Organic-inorganic membranes containing the nanoparticles of hydrated zirconium dioxide and BaFe12O19 magnetic nanoparticles were obtained. The nanoparticles were inserted into polymer matrices, they form aggregates, a size of which is up to 20 nm (active layer) and up to 2 μm (macroporous fibrous support). Larger aggregates are formed in absence of the magnetic constituent (up to 5 μm). The membranes were tested for filtration of sugar beet juice. Due to smaller particle size, the membrane containing also BaFe12O19 shows the liquid flux of 4.3×10-7-5.7×10-7 m3m-2s-1 at 2 bar and rejection towards vegetable protein of 55-87%. Regarding the membranes including no magnetic nanoparticles, these values are 3.8×10-7-5.5×10-7 m3m-2s-1and 38-77 %.**

Keywords* — *nanoparticles, membrane separation, magnetic nanocomposite, hydrated zirconium dioxide, barium ferrate.

I. Introduction

Ultrafiltration technology is widely used for removal of colloidal particles from ground and brackish water, wastewater, sea water [1]. This stage of water treatment is before reverse osmosis to prevent membrane fouling. Ultrafiltration is also applied to beverage industry, for instance, for milk skimming and effluents treatment etc. The main problem of filtration is a decrease of membrane permeability due to fouling with organics. This is especially important, when liquids of biological origin are processed.

In general, species of organic substances, microorganisms, iron oxide and silicon dioxide significantly decrease the time of filtration. The membranes need chemical regeneration that involves aggressive reagents. Frequent regeneration reduces a lifetime of the membranes. One of the ways to overcome these disadvantages is to enhance hydrophilicity of polymer membranes. As a rule, nanoparticles of inorganic ion-exchangers are used for modification of polymers. A number of inorganic compounds are applied to modifying [2]: zirconium hydrophosphate [3] (the attempt to use these materials as a filler for electromembrane processes is known [4], moreover, they are used for modifying of ion exchange resins [5]), silica [6], hydrated zirconium [3, 7] or iron oxide [8]. This approach allows one to enhance liquid permeability and anti-fouling ability without sufficient changes of membrane structure.

Magnetic particles are another type of modifier that improves functional properties of polymer membranes. The membrane containing magnetic Fe_3O_4 nanoparticles and graphene oxide particles shows high flow of pure water and high degree of rejection (up to 83.0%) [9]. Membranes containing iron nanoparticles can be used to remove copper and lead ions from wastewater [9, 10]. Adsorption capacity increases due to improved hydrophilicity on the one hand and nucleophilic functional groups on the surface of nanoparticles on the other hand. Nanocomposite membrane exhibits minimal interaction with whey protein due to its higher hydrophilicity, which leads to a polar-non-polar interaction between membrane surface and protein. This depresses membrane fouling [11].

The membranes modified with magnetic nanoparticles shows an increase in water flow due to changes in the average pore radius, porosity and hydrophilicity of the membranes. The membrane surface roughness and hydrophilicity are considered to be main factors, which minimize membrane fouling.

The aim of the work was to obtain organic-inorganic membranes containing inorganic modifier, particularly magnetic one, and to establish the effect of the filler on separation ability of the composite membranes and their stability against fouling.

II. Experiment Details

A. Membrane modifying

Ultrafiltration membranes (produced by the Institute of Physico-Organic Chemistry of the National Academy of Science of the Republic of Belarus) were used for investigations as a polymer substrate. These materials consist of macroporous substrate (non-woven polyester) and ultrathin active layer (polysulfone (PS) or polyacrylonitrile (PAN)). Further the membranes were marked according to the polymer forming the active layer. PS and PAN rejects

globular proteins, molecular mass of which is 100 and 50 kDa, respectively.

Magnetic nanoparticles (MNP) $BaFe_{12}O_{19}$ were synthesized according to [12]. In order to provide their fixation in membrane pores, hydrated zirconium dioxide (HZD) was used. First of all, sol of insoluble zirconium hydroxocomplexes was obtained from a 0.25 M $ZrOCl_2$ solution similarly to [13]. MNP were dispersed in zirconium sol and treated with ultrasound at 30 kHz. The membranes were degassed in deionized water under vacuum conditions at 343 K, and impregnated with suspension of MNP in sol. Then HZD and MNP were coprecipitated directly in the polymer with a 0.1M NH4OH solution. The membrane was dried at 50°C and cleaned with ultrasound to remove the precipitate from its outer surface. This approach, which involves impregnation of a membrane with the suspension of insoluble compounds followed by precipitation, was applied earlier to modification of ceramics [14]. For comparison, the membranes containing only HZD were obtained. In this case, the polymer matrix was impregnated with zirconium-containing sol.

Morphology of the membranes was investigated using scanning electron microscopy (SEM). Fractal dimension of aggregates in macroporous support was determined with methods of cube counting, triangulation, and power spectrum analysis similarly to [15].

Before the application of transmission electron microscopy (TEM), the active layer was separated from the macroporous substrate, and milled in the medium of liquid nitrogen.

B. Membrane testing

The experimental set-up for filtration consisted of typical elements for baromembrane separation (magnetic pump, manometer, rotameter). A divided two-compartment flow-type cell was used. An effective area of the membrane was $2.82 \cdot 10^{-3}$ m^2. Before the measurements, the membrane was pressed by means of pumping deionization water at 4 bar. The effluent volume was measured after predetermined time. Filtration was stopped, when the constant flow rate through the membrane was achieved.

Tap water containing 1 and 0.2 mol dm^{-3} Ca^{2+} and Mg^{2+} respectively was used for testing. The content of ions in permeate was determined by means of atomic absorption technique. Filtration was carried out at 2 bar. Sugar beet juice (PC "Salyvonkivskyy sugar factory") was also applied to investigations. Before testing, juice was diluted in 10 times. The content of vegetable proteins was determined in permeate using such dye as Coomassie brilliant blue G-250 [15]. Selectivity of membranes (φ), i.e. rejection of species was estimated via [1]:

$$\varphi = \left(1 - C_p / C_f\right) \times 100\% \ . \qquad (1)$$

Here C_p and C_f are the concentration of feeding solution and permeate, respectively.

III. Results and Discussion

A. Morphology of membranes

As an example, typical SEM images of the pristine PAN membrane are given in Figs. 1 a, b. It is seen that the microporous support consists of sprung fibers, a size of which is 10-20 μm. Active layer is attached to the support forming the membrane that is able to reject colloidal particles. During HZD precipitation, the particles, a size of which is up to 5 μm, are formed in the support, when MNP are absent (Fig. 1c). In the case of MNP in sol, the size of aggregate is up to 2 μm (Fig. 1d). Analysis of fractal dimension gives 2.4-2.7 indicating diffusion as a limiting stage during aggregate formation. The mechanism involves sticking of particles to a small cluster (DLA model) [17]. In our case, MNP particles are evidently additional precipitation centers.

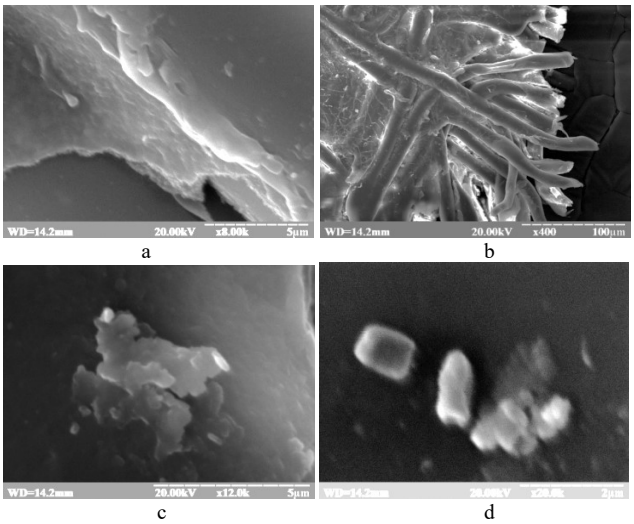

Fig. 1. SEM image of pristine (a, b) and modified (c, d) PAN membrane: active layer (a) and macroporous support (b-d). One-component HZD (c) and HZD containing MNP (c. d) were used as a modifier.

Indeed, the flux of particles (**J**) during precipitation is determined by Fick's law:

$$\mathbf{J} = D \nabla C \ , \qquad (2)$$

where D and C are the diffusion coefficient and the concentration of particles being formed. Formation of smaller particles causes increase of their concentration gradient, which moves from the outer sides of a membrane to its middle together with a precipitator. When deposition occurs, higher concentration gradient is realized for smaller particles. On the other hand, magnetic nanoparticles provide local magnetic fields inside membrane. As found for solutions of NaCl, KCl, $CaCl_2$ and Na_3PO_4, their conductivity increases under the influence of magnetic field [18]. The reason is suggested to be structuring water in hydrate shells of ions, this results in increase of their diffusion coefficient. It is possible to assume that bonded water around the particles is also structured promoting faster diffusion. Enhancement of particle movement affected by magnetic field leads to formation of smaller aggregates comparing with the case of MNP absence.

TEM image of the active layer (Fig. 2a) shows very small aggregates of nanoparticles (up to 20 nm). Dark contrast spots evidently correspond to MNP, grey traces are related to HZD.

For comparison, the image for MNP is also given. The shape of nanoparticles is seen to be close to globular. A size of the primary particles is about 10 nm. The size of aggregates embedded to the active layer corresponds to pore size of the polymer according to its rejection ability towards proteins, molecular mass of which is 50 kDa.

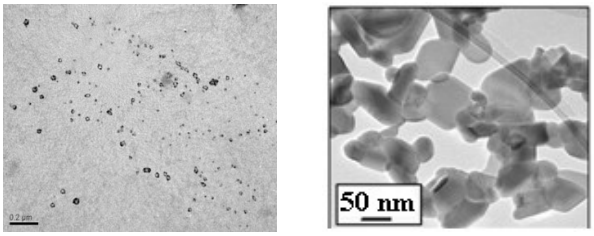

a b

Fig. 2. TEM image of active layer of PAN membrane containing HZD and MNP (a). The image of MNP that are outside the membrane is also given (b).

B. Water fitration. Secondary active layer

Fig. 3 illustrates a volume of permeate (V) as a function of time of water filtration (τ). As seen, the dependencies are linear. This allows us to estimate water flux (J) as:

$$J=\frac{dV}{d\tau}\frac{1}{A}, \qquad (3)$$

where A is the membrane area. The calculations were made from the slopes of the lines to the abscissa axis, the results are given in Table 1.

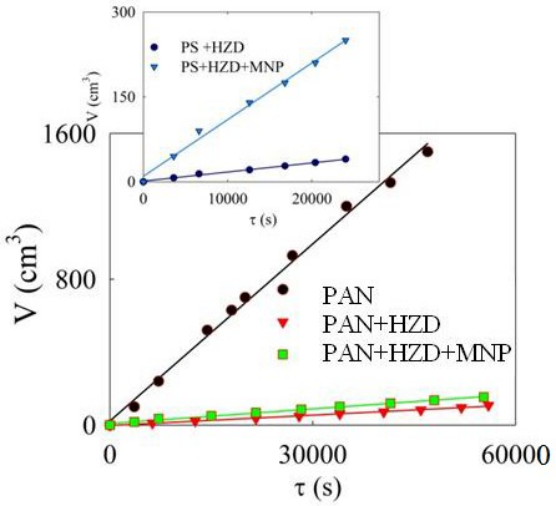

Fig. 3. Permeate volume as a function of time of water filtration through the PAN membrane. Insertion: it is the same for the PS membrane.

TABLE I. FILTRATION OF LIQUIDS AT 2 BAR

Membrane	Water		Sugar beet juice	
	J (m^3m^{-2} s^{-1})	φ (%), Ca^{2+}, Mg^{2+}	J (m^3m^{-2} s^{-1})	φ (%), VP
PAN	1.1×10^{-5}	6-7	1.1×10^{-6}	16-26
PAN+HZD	5.9×10^{-7}	8-19	3.8×10^{-7}	58-77
PAN+HZD +MNP	9.5×10^{-7}	7-20	4.3×10^{-7}	78-87
PS	2.3×10^{-5}	2-3	2.4×10^{-6}	6-13
PS+HZD	5.7×10^{-7}	5-7	5.5×10^{-7}	38-49
PS+HZD+ MNP	3.6×10^{-6}	5-6	5.7×10^{-7}	55-60

As seen, the PAN membrane containing HZD and MNP shows lower permeate flux than the pristine membrane. due to filling of the polymer pores. At the same time, rejection of hardness ions becomes higher due to decrease of pore size in the active layer and charge effect. The φ values are similar for the membranes containing MNP and free from them. At the same time, the PS membranes show higher values of fluxes and lower rejection of Ca^{2+} and Mg^{2+}. It means that the PAN polymer membrane, which is characterized by smaller holes in active layer, is more attractive for modifying.

The inorganic particles form "secondary active layer" inside the polymer pores: this layer determines water flux and rejection ability of the membrane. Its thickness (l) was calculated from Kozeny-Carman equation [19]:

$$\frac{\Delta P}{l}=\frac{180\mu\left(1-\varepsilon^2\right)}{\Phi^2 d^2\varepsilon^3}J\ , \qquad (4)$$

where ΔP is the pressure drop, ε is the porosity (0.33 for compact bed of globules), Φ is the particle sphericity (it is assumed that $\Phi = 1$), d is the particle diameter (≈10 nm), μ is the dynamic viscosity (9×10^{-3} Pa·s at 298 K). The calculations give $l \approx 0.58$ μm both for the PS and PAN membranes containing HZD. This value is comparable with a thickness of active layer of the membrane. Regarding the membranes containing also MNP, l = 95 nm (PAN) and 0.87 μm (PS). Thus, thinner "secondary active layer" is formed in the polymer matrix containing smaller pores. In the case of PS, the nanosized inorganic particles are dispersed through the polymer active layer.

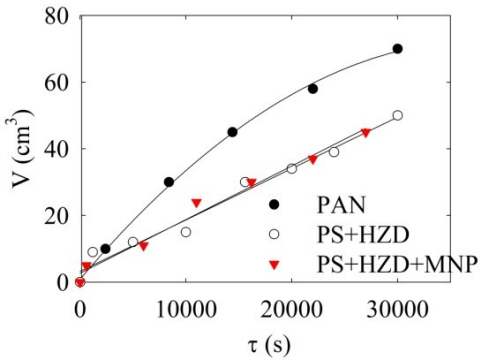

Fig. 4. Permeate volume *vs* time of filtration of sugar beet juice.

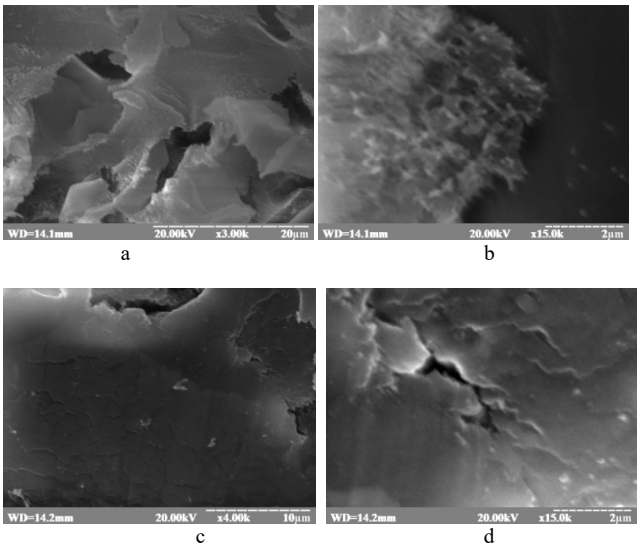

a b c d

Fig. 5. SEM images of the samples after filtration of sugar beet juice: pristine PAN membrane (a, b), membrane modified with HZD (c), HZD and MNT (d).

C. Filtration of sugar beet juice

In all cases, filtration of sugar beet juice caused its clarification. Vegetable proteins partially penetrated into the permeate (see Table 1). Modifying was shown to improve ability of the membranes to reject this valuable component. Higher φ values were found for the membranes containing MNT. As seen from Fig. 4, the $V - \tau$ dependences can be fitted with linear functions (organic-inorganic membranes) or tend to plateau formation (pristine membrane).

The depression of filtration is due to fouling with organics: the precipitate is seen as a web-like patina (Fig. 5). At the same time, the outer surface of the organic-inorganic membrane remains clean.

IV. Conclusions

When hydrated zirconium dioxide is deposited in ultrafiltration polymer membranes, aggregates of the nanoparticles are formed both in macroporous support and active layer. MNP provides formation of smaller HZD particles. Fractal analysis shows the DLA model of particle formation. The function of MNP is assumed to accelerate diffusion of HZD nanoparticles being precipitated. This depresses enlargement of the aggregates. As a result of modifying, the composite membrane shows slight improvement of rejection of hardness ions and much higher rejection of vegetable proteins comparing with pristine membranes. The modifying effect is most expressed for the PAN polymer membrane, which is characterized by smaller pores through its active layer comparing with the PS membrane. The composites also demonstrate stability against fouling with organics due to additional hydrophilization of polymer support. The membranes can be recommended for water treatment and processing of feedstock and wastes of food industry.

Acknowledgment

The work was performed within the framework of the project entitled "Baro- and electromembrane processes in technologies for purification of liquid media produced by food technologies" (grant number 0117U001247 supported by the Ministery of Education and Science of Ukraine). The work was also supported by the joint Ukrainian-Belorussian project that is called "Development of composite ultra- and nanofiltration membranes with predetermined functional properties for complex processing of wastes of food industry" (supported by the National Academy of Science of Ukraine and by the National Academy of Science of Belarus). The authors thank Dr. S. Scherbakov (M.G. Kholodnii Institute of Botany of the NAS of Ukraine) for his support of investigation using electron microscopes.

References

[1] S. Adham, Development of a Microfiltration and Ultrafiltration Knowledge Base, New York: AWWA, 2005.

[2] M. Zahid, A. Rashid, S. Akram, Z. A.D. Rehan, and W.Razzaq, "A Comprehensive Review on Polymeric Nano-Composite Membranes for Water Treatment," J. Membr. Sci. Technol, vol. 8, no. 1, pp.1–20, 2018.

[3] V. G. Myronchuk et al., "Organic-inorganic membranes for filtration of corn distillery," Acta Period. Technol., vol. 47, pp. 153–165, 2016.

[4] Yu. S. Dzyazko, L. M. Rozhdestvenskaya, and A. V. Pal'chik, "Recovery of Nickel Ions from Dilute Solutions by Electrodialysis Combined with Ion Exchange," Russ. J. Appl. Chem., vol. 78, no. 3, pp. 414–421, 2000.

[5] Yu. S. Dzyazko, L. N. Ponomaryova, Yu. M. Volfkovich, V. V. Trachevskii, and A. V. Palchik, "Ion-exchange resin modified with aggregated nanoparticles of zirconium hydrophosphate. Morphology and functional properties," Micropor. Mesopor. Mater., vol. 198, pp. 55–62, 2014.

[6] J. Chen, et al., "Preparation and characteriztion of PES-SiO_2 organic-inorganic composite ultrafiltration membrane for raw water treatment," Chem. Eng. J., vol. 168, vol. 3, pp. 1272–1278, 2011.

[7] R. Pang et al., "Preparation and characterization of ZrO_2/PES hybrid ultrafiltration membrane with uniform ZrO_2 nanoparticles," Desalination, vol. 332, no. 1, pp. 60–66, 2014.

[8] Z. Rahimi, A. A. Zinatizadeh, and S. Zinadini, "Preparation and characterization of high antifouling ultrafiltration PES membrane using OCMCS-Fe_2O_3 for application in MBR treating wastewater," J. Appl. Res. Water Wastewater, vol. 1, pp. 13–17, 2014.

[9] Y. Huang, et al., "Magnetic field induced orderly arrangement of Fe_3O_4/GO composite particles for preparation of Fe_3O_4/GO/PVDF membrane," J. Membr. Sci., vol. 548, no. 15, pp. 184–193, 2018.

[10] N. Ghaemi et al., "Polyethersulfone membrane enhanced with iron oxide nanoparticles for copper removal from water: Application of new functionalized Fe_3O_4 nanoparticles," Chem. Eng. J., vol. 263, pp. 101–112, 2015.

[11] D. Quemener, L. Upadhyaya, M. Semsarilar, and A. Deratani, "Nanocomposite Membranes with Magnesium, Titanium, Iron and Silver Nanoparticles – A Review," J. Membr. Sci. Res., vol. 3, no. 3, pp. 187–198, 2017.

[12] A. G. Belous, O. I. V'yunov, E. V. Pashkova, V. P. Ivanitskii, and O. N. Gavrilenko, "Mössbauer Study and Magnetic Properties of M-Type Barium Hexaferrite Doped with Co + Ti and Bi + Ti Ions," J. Phys. Chem. B, vol. 110, pp. 26477–26481, 2006.

[13] Yu. Dzyazko, Yu. Volfkovich, V. Sosenkin, N. Nikolskaya, and Yu. Gomza "Composite inorganic membranes containing nanoparticles of hydrated zirconium dioxidefor electrodialytic separation," Nanoscale Res. Lett., vol. 9, no. 1, p. 271, 2014.

[14] Yu. S. Dzyazko, A. S. Rudenko, Yu. M. Yukhin, A. V. Palchik, and V. N. Belyakov, "Modification of ceramic membranes with inorganic sorbents. Application to electrodialytic recovery of Cr(VI) anions from multicomponent solution," Desalination, vol. 342, pp. 43–51, 2014.

[15] C. Douketis, Z. Wang, T. L. Haslett, and M. Moskovits, "Fractal character of cold-deposited silver films determined by low-temperature scanning tunneling microscopy," Phys. Rev. B, vol. 51, no. 16, pp. 11022–11032, 1995.

[16] H. K. Mæhre, L. Dalheim, G. K. Edvinsen, E.O. Elvevoll, and I.-J. Jensen, "Protein Determination—Method Matters," Foods, vol. 7, no. 1, pp. 5, 2018.

[17] P. Meakin, "Progress in DLA research," Phys. D: Nonlimear Phenomena, vol. 86, no. 1–2, pp. 104–112, 1995.

[18] L. Holysz, A. Szczes, and E. Chibowski, "Effects of a static magnetic field on water and electrolyte solutions," J. Colloid Interface Sci., vol. 316, pp. 996–1002, 2007.

[19] W. L. McCabe, J. C. Smith, and P. Harriot, Unit Operations of Chemical Engineering, New York: McGraw-Hill, 2005.